COVER SHEET

Title: ***Fire Behavior of Two-Way Post-Tensioned Concrete Slabs Provided with Bonded Tendons: an Experimental Study.***

Authors: Li Zhang
Ya Wei
Francis Tat Kwong Au
Jing Li

PAPER DEADLINE: ****MARCH 11, 2016****

PAPER LENGTH: ****8 PAGES (Maximum) ****

INQUIRIES TO: **Papers to be sent to editors (*Contact Editors if further contact information necessary*).**

Dr. Maria E. Moreyra Garlock
Associate Professor
Princeton University

E-mail: mgarlock@princeton.edu

ABSTRACT

Fire tests of three reduced-scale two-way post-tensioned concrete slabs with bonded tendons were carried out. This study was intended to investigate the influence of the layout of prestressing tendons, prestressing force and concrete spalling on the structural response of two-way post-tensioned concrete slabs with bonded tendons in fire. The material used to fabricate the specimens, the phenomena observed during the tests, the temperature distributions, the deflections and occurrence of concrete spalling were investigated.

INTRODUCTION

Post-tensioned concrete slabs are common structural components in buildings to achieve large span-to-depth ratios and economy. They may be one-way or two-way. A typical one-way slab has an aspect ratio of 2 or above and is usually supported at the two longer opposite sides. A two-way slab has an aspect ratio below 2 but there may be more variations. It may be supported by beams at all four sides of the perimeter or supported by columns at the four corners as in the case of flat slab.

Previous studies have provided comprehensive knowledge of the behavior of one-way post-tensioned concrete slabs in fire [1-5]. Work has also been done on the structural fire performance of two-way reinforced concrete slabs [6] and two-way post-tensioned slabs with unbonded tendons [7], but little of such work has been done on two-way post-tensioned concrete flat slabs with bonded tendons. The present experimental study aims to explore the structural behavior of two-way bonded post-tensioned concrete slab at elevated temperatures with particular attention to concrete spalling, failure mode, etc.

Li Zhang, Department of Civil Engineering, the University of Hong Kong, Pok Fu Lam Road, Hong Kong.
Ya Wei, Department of Civil Engineering, the University of Hong Kong, Pok Fu Lam Road, Hong Kong.
Francis Tat Kwong Au, Department of Civil Engineering, the University of Hong Kong, Pok Fu Lam Road, Hong Kong.
Jing Li, School of Civil Engineering and Transportation, South China University of Technology, Wushan Road, Guangzhou, Guangdong Province, China

TEST PROGRAM

Dimensions and Material Properties of Specimen

Three specimens of post-tensioned two-way concrete flat slab provided with bonded tendons were fabricated for fire testing. The specimens were designed to a reduced scale mainly according to ACI318-08 [8] and BS EN 1992-1-1 [9] to satisfy the available space inside the furnace. Each slab specimen comprised a central rectangular area bounded by four columns at the corners of that area and cantilever panels outside the rectangular area as shown in Figure 1. The slab thickness and concrete cover were 95mm and 10mm respectively. Linear variable differential transducers (LVDTs) and thermocouples were placed at critical locations to measure the displacements and temperature distributions respectively.

The tendons were provided with curved profiles as shown in Figure 2. For the distributed-distributed tendon arrangements, tendons X1 to X6 employed were given “Profile-A1”. Tendons Y1, Y2, Y5 and Y6 employed were given “Profile-A2” while Y3 and Y4 employ were given “Profile-A3”. For the distributed-banded tendon arrangements, tendons X1 to X6 employed were given “Profile-B1”. Tendons Y1, Y2, Y5 and Y6 employed were given “Profile-B2” while tendons Y3 and Y4 employed were given “Profile-B3”. The tendons were stressed to the target levels expressed as percentage of the corresponding “yield strength” as shown in Table 1. The tendon arrangement and design load ratio are also given in Table 1.

C40 and C60 concrete mixes were used in the base and columns respectively. Grade 1860 prestressing steel strands to GB/T 5224 with diameter of 12.7 mm and nominal cross sectional area of 98.7 mm^2 were employed as prestressing tendons. Circular corrugated steel ducts originally with diameter of 40 mm, thickness of 0.3 mm and yield strength 195 MPa were flatted before use. The concrete used in the fabrication of the slab was C60 self-consolidating concrete with aggregate size of 5-10mm. The 28-day cube strength and the moisture content were shown in Table 2. The grout was produced with 42.5R cement with water to cement ratio of 0.4, providing a 28-day compressive strength of 42.6 MPa.

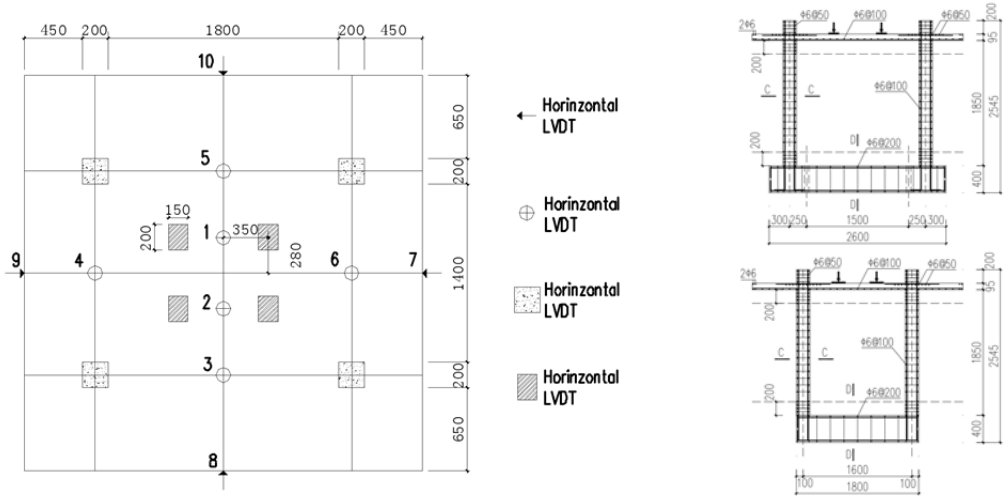

(a) Plan view (b) Side view

Figure 1. Dimensions of specimen (unit: mm)

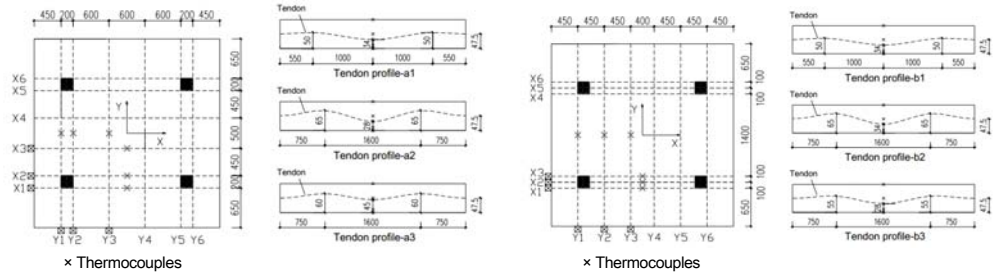

(a) Distributed-distributed (b) Distributed-banded

Figure 2. Tendon distribution and profile (unit: mm)

TABLE 1. DESIGN TEST CONDITIONS OF SPECIMENS

Specimen	Tendon arrangement	Bond condition	Target prestressing level	Design load ratio
1	Distributed-distributed	Bonded	37%	25%
2	Distributed-distributed	Bonded	50%	50%
3	Distributed-banded	Bonded	50%	25%

TABLE 2. PROPERTIES OF SPECIMENS

Specimen	Force of tendons		Load (kN)	Concrete strength (kN)		Concrete moisture content (%)
	Target force (kN)	Measured force (kN)		28-day	Test day	
1	67.9	64.7	43.4	61.5	53.9	2.49
2	91.8	94.5	85.7	61.5	53.0	2.10
3	91.8	94.8	43.4	61.5	53.2	2.02

Test Facilities

The temperature in the furnace was controlled by a computer and monitored by 12 thermocouples to ensure the required temperature. The load applied by a hydraulic jack was transferred through steel beams onto 4 loading areas on the slab by 4 spreaders as shown in Figure 1(a). Ten LVDTs were placed at different locations as shown in Figure 1(a). The vertical LVDTs were denoted as VD-1 to VD-6 and the horizontal LVDTs were denoted as HD-7 to HD-10. Positive LVDT measurements refer to either the vertical downward displacement or horizontal outward displacements.

The thermocouples were denoted according to their locations as shown in Figure 2. Taking the thermocouples at the middle of tendon Y3 for example, Y3-T, Y3-M, Y3-B, Y3-P, Y3-S, Y3-Dt and Y3-Db denoted the thermocouple located at the top surface, the mid-depth, the bottom surface, the prestressing tendons, the reinforcing steel, the top surface of the duct and the bottom surface of the duct respectively. Centroid-B denoted the thermocouple located at the bottom surface of the centroid of the panel.

Test Procedure

The test setup was shown in Figure 3. The soffit of the central panel within the rectangle defined by the four columns will be heated while the cantilever parts, the columns and the base of the specimens were protected with fireproof material after the fabrication of specimens. The transient state method was adopted where the load was constantly acting on the specimen when the temperature of the specimen was elevated until structural failure. The measured temperature curves of tests were compared to the standard fire curve of ISO 834 as shown in Figure 3(c).

(a) Furnace (b) Loading setup (c) Temperature curves

Figure 3. Test Setup and measured temperature curves

RESULTS AND DISCUSSIONS

Observations

In test 1, continuous noise due to concrete spalling was heard from 5 minutes after ignition to the end of the test. Cracks were first observed in line with tendons X3 and Y4 near the load spreader accompanied by water seepage due to evaporation. At around 40 minutes, a “big bang” was heard and a through hole was observed at the intersection of tendons X4 and Y4, after which the test was terminated.

In test 2, similar to test 1, continuous noise due to concrete spalling was heard from 5 minutes after ignition to the end of the test except that the noise due to concrete spalling was more intensive. A “big bang” was heard due to the crushing of part of the concrete at the top surface at 34 minutes.

In test 3, the test was relatively quiet compared to the previous tests. Noise was first heard at 7 minutes. All the noise due to concrete spalling occurred in the first 19 minutes. The first crack was observed parallel to and near tendon Y4. At 50 minutes, all the water at the top surface had evaporated. The specimen was heated for 120 minutes without apparent concrete spalling at the top surface, which exceeded the design fire resistance of 90 minutes in accordance with BS EN 1992-1-2 (2004) [9].

3.2 Temperature Distribution

Figure 4 shows the temperature-time curves of the thermocouples in the central slab panel. Comparing the temperatures at different levels, e.g. X3-B, X3-S, X3-P, X3-M and X3-T in Figure 4(a), shows different heating rates depending on the distance from the slab soffit, which clearly reflects the poor thermal conductivity of concrete. The temperatures of X3-P in Figures 4(a)-(c) were higher than those of Y3-P because of the smaller distance of X3-P to the soffit compared with that of Y3-P. In particular, the temperature of X3-B in Figure 4(a) was higher than that of Y3-B because of more severe continuous concrete spalling at the corresponding location, leading to thinner concrete cover.

Figures 4(a)-(b) show sharp increases of temperatures around 10 to 15 minutes after ignition, which indicate the occurrence of severe concrete spalling at the soffit, almost directly exposing the thermocouples to fire. The temperature curves in Figure 4(c) are relatively smooth and free of any sudden jump because of the milder concrete spalling of specimen 3 as compared to the first two specimens. Moreover, the heating rates of the top surface of specimens also increased gradually because of the concrete spalling and hence shorter path of heat transfer.

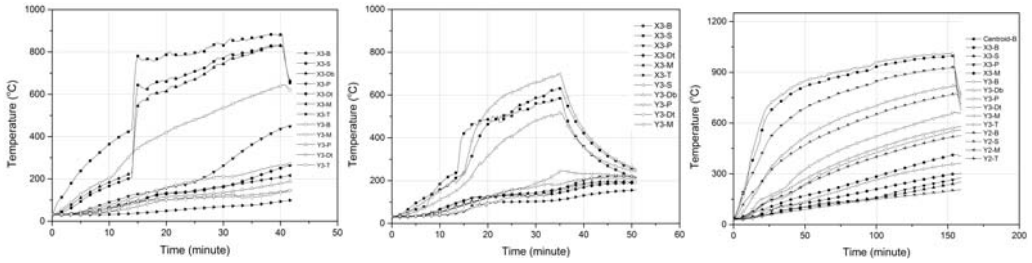

(a) Specimen 1 (b) Specimen 2 (c) Specimen 3

Figure 4. Temperature distributions of specimens

3.3 Structural Responses

The vertical displacements at critical locations are used to describe the structural responses of the specimens. The vertical responses were dominated by thermal bowing caused by the thermal gradients across the depth of the slab and hence differences in thermal expansion [10] combined with the thermal thrust forces provided by restraints [11]. The horizontal displacements were dominated by thermal expansion of the specimens. Furthermore, the variations of vertical and horizontal displacements were related to the degradation of mechanical properties of concrete, steel reinforcement and prestressing tendons as well as their thermal relaxation with the increase in temperature. The severity of concrete spalling also contributed to the increase in camber of slab due to loss of self-weight and reduced stiffness as the temperature increased.

Among various vertical displacements of Specimen 1 as shown in Figure 5(a), displacements VD-1 and VD-2 had a relatively rapid increase in the first 6 minutes due to increasing thermal gradient as temperature rose, while VD-3, VD-4 and VD-6 had relatively slower increase, showing that thermal gradient dominated the vertical displacements at this stage. Afterwards, the rate of increase of vertical displacements reduced gradually while the thermal gradient decreased and the thermal thrust increased. The vertical displacements reached the peak at around 10 minutes and started to decrease until the end of the test, probably because severe concrete spalling led to reduced self-weight and stiffness of the slab. The curved prestressing tendons gradually dominated the load carrying mechanism and caused more camber.

The vertical displacements of Specimen 2 as shown in Figure 5(b) have similar trends as those of Specimen 1. The LVDT measurements indicate relatively symmetrical deformation pattern of the specimen. The vertical displacements at VD-3 and VD-5 were larger than those at VD-4 and VD-6 because of the larger span in the X direction and hence smaller flexural stiffness. The maximum vertical

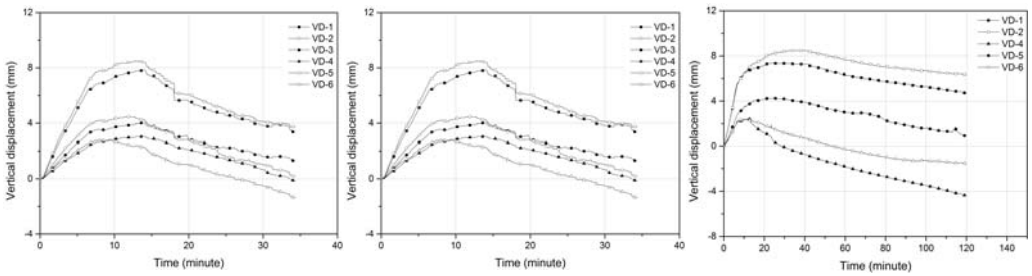

(a) Specimen 1 (b) Specimen 2 (c) Specimen 3

Figure 5. Vertical displacements of specimens

displacements were reached at around 13 minutes when sudden increase in temperature of X3-B occurred as shown in Figure 4(b), confirming the effects of concrete spalling on the structural response.

Figure 5(c) shows the vertical displacements of Specimen 3 that has undergone a fire test of over 120 minutes. The vertical displacements of VD-1 and VD-2 rose in the first 30 minutes and dropped afterwards. The vertical displacements of VD-1, VD-2 and VD-5 remained positive at 120 minutes while those of VD-4 and VD-6 were negative, implying that the camber effect was more significant at VD-4 and VD-6. This was consistent with the tendon layout as shown in Figure 2(b), since there were 3 tendons close to VD-4 and VD-6, but fewer tendons close to VD-1, VD-2 and VD-5. The localized upward pressure provided by the three adjacent tendons caused the upward displacements of VD-4 and VD-6.

3.4 Concrete Spalling

After the fire tests, the cracks and concrete spalling were closely examined. Figure 6 shows the concrete spalling at the soffit of Specimens 2 and 3. Both Specimens 1 and 2 had severe concrete spalling, while that of Specimen 3 was less severe. Concrete spalling at elevated temperature obviously influenced the structural integrity and temperature distribution, possibly causing premature failure.

The lost area at the soffit of Specimen 2 caused by concrete spalling accounted for more than 60% of the central panel while the depth of concrete spalling in most part was over 50mm, as shown in Figure 6(a). The majority of reinforcing bars and tendons X3, X4 and Y4 were exposed to fire. As no ruptured reinforcing bars were found, the tensile stresses in the bars should be relatively low at the corresponding temperatures. The through hole occurred near the intersection between tendons X4 and Y4 where one of the load spreader sat. Obviously before the formation of through hole by severe spalling, the concrete depth of the heated area was reduced, thus weakening the concrete seriously. Afterwards the adjacent concentrated load failed the thin layer of the concrete by combined flexure and shear.

The severity of concrete spalling in Specimen 3 as shown in Figure 6(b) was much less severe as compared to Specimen 1 and 2. The depth of concrete spalling was around the thickness of concrete cover (i.e. 10mm) and cracks in line with tendons X3 and X4 were also found at the soffit. A few reinforcing bars were exposed but the tendons were still well protected.

(a) Test 2 (b) Test 3

Figure 6. Concrete spalling of Tests 2 and 3

3.4 Discussions

The integrity of post-tensioned concrete slab is a major concern as it affects the structural behavior. The top surface of Specimen 1 to 3 sustained the fire for 40 minutes, 34 minutes and over 120 minutes respectively, while the soffit suffered different degrees of concrete spalling.

Only Specimen 3 sustained the desirable structural fire resistance with satisfactory integrity. One of the critical factors contributing to massive concrete spalling was probably the highest heating rate of test 2 at the early stage as shown in Figure 3(b). The higher the heating rates, the greater the probability of concrete spalling as concluded in previous studies on the fire resistance of concrete structures [12-14].

Another factor affecting the possible loss of concrete integrity at the soffit was the compressive concrete stresses at the soffit of panel center induced by restrained thermal expansion and post-tensioning. Specimens with distributed-banded tendon layout had tendons Y3 and Y4 located near the center of central panel while the other specimens with distributed-distributed tendon layout had tendons X3, X4, Y3 and Y4 located near the center. Additionally with the interweaving ducts near the center of specimen with distributed-distributed tendon layout, the reduced depth of concrete at duct intersections weakened the slab there to certain extent.

The difference between the largest displacement and the displacement at the end of the test can be considered to result from spalling and stiffness. Specimens 1, 2 and 3 had displacement differences of 7.95, 4.57 and 2.39mm. The value of Specimen 3 was the smallest because its stiffness was the largest among the specimens, which restrained the deformation of the bonded tendons.

The increased camber helped reduce the tensile stress in the reinforcing bars so that they could survive the reduction in tensile strength at elevated temperatures. The upper layer of concrete was mainly under tension perpendicular to the tendon as proven by the crack appearance in line with the tendons.

4 CONCLUSIONS

Three specimens of post-tensioned concrete flat slab with bonded tendons were tested at elevated temperatures. The specimens were designed with different load ratios, prestress levels and tendon layouts. The first two specimens suffered severe concrete spalling while the other one retained satisfactory integrity. Based on the test results, some conclusions can be drawn as follows:

(a) Concrete spalling at elevated temperatures severely affected the integrity of structure and gave rise to temperature and stress redistribution, which could lead to progressive concrete spalling.
(b) Further camber occurred after severe concrete spalling and hence partial loss of self-weight, thus releasing the constraints of the bonded tendons and weakening the stiffness of slab.
(c) The concrete spalling at the soffit can be attributed to the reduced compressive strength of concrete at elevated temperature coupled with the increasing compressive stress in concrete as induced by retrained thermal expansion and prestressing.
(d) While prestressing can contribute to concrete spalling by inducing large compressive stresses at the soffit, later in the heating process it can also reduce the tension in reinforcing bars thereby protecting them to certain extent.

REFERENCES

[1] Bailey, C.G. and E. Ellobody. 2009. “Fire tests on unbonded post-tensioned one-way concrete slabs,” *Magazine of Concrete Research*, 61(1), 67-76.

[2] Bailey, C.G. and E. Ellobody. 2009. “Fire tests on bonded post-tensioned concrete slabs,” *Engineering Structures*, 31(3), 686-696.

[3] Bailey, C.G. and E. Ellobody. 2009. “Comparison of unbounded and bonded post-tensioned concrete slabs under fire conditions,” *The Structural Engineer*, 87(19), 23-31.

[4] Ellobody, E. and C.G. Bailey. 2009. “Modelling of unbonded post-tensioned concrete slabs under fire conditions,” *Fire Safety Journal*, 44(2), 159-167.

[5] Ellobody, E. and C.G. Bailey. 2008. “Modelling of bonded post-tensioned concrete slabs in fire,” *Structures and Buildings*, 161(6), 311-323.

[6] Moss, P. J., R. P. Dhakal, G. Wang, and A. H. Buchanan. 2008. “The fire behaviour of multi-bay, two-way reinforced concrete slabs,” Engineering Structures 30(12), 3566-3573.

[7] Wei, Y., F.T.K. Au, J. Li and N.C.M. Tsang, 2014. “Structures in Fire,” presented at the 8th International Conference on Structures in Fire, June 11-13, 2014.

[8] ACI 318-08. 2008. *Building Code Requirements for Structural Concrete and Commentary*. ACI Standards, American Concrete Institute, Farmington Hills, MI, U.S.A.

[9] BS EN 1992-1-2. 2004. *Eurocode 2: Design of concrete structures - Part 1-2: general rules – structural fire design*. British Standards Institution, London, UK.

[10] Usmani A.S., J.M. Rotter, S. Lamont, A.M. Sanad and M. Gillie. 2001. “Fundamental principles of structural behaviour under thermal effects,” *Fire Safety Journal*, 26(8), 721-744.

[11] Lim, L., A. Buchanan, P. Moss and J. Franssen. 2004. “Computer modelling of restrained reinforced concrete slabs in fire conditions,” *Journal of Structural Engineering*, 130(12), 1964-1971.

[12] Ali F., A. Nadjai, G. Slikock and A. Abu-Tair. 2004. “Outcomes of a major research on fire resistance of concrete columns,” *Fire Safety Journal*, 39(6), 433-445.

[13] Chung J.H. and G.R. Consolazio. 2005. “Numerical modeling of transport phenomena in reinforced concrete exposed to elevated temperatures,” *Cement and Concrete Research*, 35(3), 597-608.

[14] Gamal A. and J. Hurst. 1995. “Modeling the behavior of concrete slabs subjected to the ASTM E119 standard fire condition,” *Journal of Fire Protection Engineering*, 7(4), 125-132.